



Folic acid-modified liposomal drug delivery strategy for tumor targeting of 5-fluorouracil

Eskandar Moghimipour^{a,b}, Mohsen Rezaei^c, Zahra Ramezani^a, Maryam Kouchak^a,
Mohsen Amini^d, Kambiz Ahmadi Angali^e, Farid Abedin Dorkoosh^{f,g}, Somayeh Handali^{a,*}

^a Nanotechnology Research Center, Ahvaz Jundishapur University of Medical Sciences, Ahvaz, Iran

^b Cellular and Molecular Research Center, Ahvaz Jundishapur University of Medical Sciences, Ahvaz, Iran

^c Department of Toxicology, Faculty of Medical Sciences, Tarbiat Modares University, Tehran, Iran

^d Department of Medicinal Chemistry, Faculty of Pharmacy, Tehran University of Medical Sciences, Tehran, Iran

^e Department of Biostatistics, School of Public Health, Ahvaz Jundishapur University of Medical Sciences, Ahvaz, Iran

^f Department of Pharmaceutics, Faculty of Pharmacy, Tehran University of Medical Sciences, Tehran, Iran

^g Medical Biomaterial Research Centre (MBRC), Tehran University of Medical Sciences, Tehran, Iran

ARTICLE INFO

Keywords:

5-Fluorouracil
Liposome
Folic acid
ROS
Cancer

ABSTRACT

The aim of this study was to develop a liposomal formulation to selectively target cancer cells. Liposomes were prepared using thin layer method and folic acid (FA) was applied for targeted delivery of 5FU to cancer cells. Liposomes prepared were characterized for encapsulation efficiency (EE%), morphology and their particle size. Cellular uptake, cytotoxicity study and ROS production were evaluated using CT26 cell line. Hemolysis test was performed on rat red blood cells (RBCs). Moreover, the efficacy of targeted liposomes were investigated by in vivo antitumor activity and tissue toxicities were studied by histological examination. The EE% and average particle size of liposomes were $67.88 \pm 1.84\%$ and 114.00 ± 4.58 nm, respectively. TEM image revealed that liposomes were spherical in shape. Targeted liposomes showed higher cellular uptake, lower IC₅₀ (12.02 μM compared to 39.81 μM for liposomal 5FU and 39.81 μM for free 5FU) and higher ROS production than free drug (62,271.28 vs 2369.55 fluorescence intensity) on cancer cells. Results of hemolysis assay confirmed the blood biocompatibility of the liposomes. Moreover, folate targeted liposomes showed better tumor inhibition than free drug (88.75 mm³ tumor volume vs 210.00 mm³) and no tissue abnormalities were found in histological examination. It can be concluded that folate targeted liposomes provide an effective and safe strategy for colon cancer targeted chemotherapy.

1. Introduction

5-Fluorouracil (5FU), a pyrimidine analog is a cytotoxic drug which is extensively used in the treatment of a variety of cancers such as colon, breast, brain, ovary, head, neck and liver cancer (Mattos et al., 2016). 5FU interferes with DNA synthesis and acts as a thymidylate synthase inhibitor. Although its efficiency, due to short half-life (6–20 min), wide distribution, and side effects such as cardiac toxicity, dermatitis and damage of the central nervous system limit its medical applications. To overcome these limitations, it is a need to develop a drug delivery system for 5FU (Cheng et al., 2012; Nair et al., 2011).

By choosing a proper drug delivery system, controlled and targeted access of drug delivery to the site of tumor, decreased drug clearance and reduced systematic side effects may be provided (Pereira et al., 2016). Liposomes are extensively considered as drug carriers for a wide

range of drugs due to biocompatibility, biodegradability, capability to entrap both hydrophilic and hydrophobic drugs, nontoxic and lack of immune system activation (Deshpande et al., 2013; Nogueira et al., 2015).

The employment of nano-particles (NPs) in cancer treatment is based on their enhanced permeability and retention (EPR) effect to tumor tissues (Nair et al., 2011). Due to abnormal leaky vasculature and impaired lymphatic drainage around the tumors, NPs can be penetrated in the tumor tissue and release the drug at specific locations; as a result, reduce the exposure to normal tissues, and decrease the side effects (Nair et al., 2011; Nogueira et al., 2015). Nevertheless, since EPR effect is affected by many factors such as tumor location, amount of infiltration by macrophages, as well as pore size of tumor vessels, the passive targeting is limited to some types of tumors. Furthermore, EPR effect is only restricted to some solid tumors which are larger than

* Corresponding author.

E-mail address: handali.somayeh@gmail.com (S. Handali).

approximately 4.6 μm in diameter (Nogueira et al., 2015). In order to overcome the drawbacks associated with passive targeting, active targeting can also be utilized. For enhancing cell specific and intracellular delivery, NPs can be further modified with targeting ligands (Chen et al., 2016). Antibodies, carbohydrates, peptides, folic acid (FA) and transferrin are among the several ligands to target cancer cells (Deshpande et al., 2013; Nogueira et al., 2015). FA, a hydrophilic B-complex vitamin can be considered as targeting ligand due to its unique property including nontoxic, small size, stable in storage and in circulation, compatibility with a variety of organic and aqueous solvents, inexpensive as well as can be easily modified (Gao et al., 2015; Shmeeda et al., 2006; Wang et al., 2013). The folate receptors (FRs) are highly expressed in many types of cancer while its expression is limited in normal cells (Fasehee et al., 2016; Laha et al., 2015; Yin et al., 2013). The aim of present study was to prepare folic acid targeted liposomes for delivery of 5FU and evaluation of cytotoxicity in vitro and in vivo.

2. Materials and methods

5-Fluorouracil (5FU) and soya phosphatidyl choline (PC) were obtained from Acros, USA. Distearoylphosphatidylethanolamine (DSPE) was purchased from Lipoid, Germany. *N*-hydroxysuccinimide (NHS), triethylamine (TEA) and cholesterol were acquired from Merck, Germany. Metronidazole kindly donated by Pars Darou Pharmaceutical Co., Iran. Poly (ethylene glycol) and 2-aminoethyl ether acetic acid (NH₂-PEG-COOH) and folic acid (FA) were provided from Sigma-Aldrich, Germany. 1-Ethyl-3-(3-dimethylaminopropyl) carbodiimide (EDC) was obtained from Alfa Aesar, Germany. 4, 6-Diamidino-2-phenylindole (DAPI), paraformaldehyde and 5 (6) - carboxyfluorescein (CF) were purchased from Sigma-Aldrich, Germany.

CT26 (murine colon carcinoma) cell lines were obtained from National Cell Bank of Iran (NCBI), Pasteur Institute of Iran. Roswell Park Memorial Institute (RPMI) 1640 medium and fetal bovine serum (FBS) were obtained from Gibco, USA. Penicillin-streptomycin, 3-(4, 5-dimethyl-2-thiazolyl)-2, 5-diphenyl tetrazolium bromide (MTT) and 2', 7'-dichlorofluorescein diacetate (DCFDA) were purchased from Sigma-Aldrich, Germany. Male BALB/c mice and male Wistar rats were obtained from the Pasteur Institute of Iran. Other chemicals and solvents were of analytical grade and acquired from Merck, Germany.

2.1. Preparation of liposomes

Detailed synthesis procedure of FA-PEG-DSPE is under consideration for publication elsewhere (data not shown here). Briefly, folic acid dissolved in methanol containing TEA, then EDC and NHS were added and was stirred for 4 h. The activated folic acid and NH₂-PEG-COOH incubated for 48 h at room temperature. Solvent was evaporated and the remained yellow color product suspended in deionized water. Thereafter, the resultant suspension was dialyzed against deionized water and the final product (FA-PEG-COOH) was freeze-dried. FA-PEG-COOH then dissolved in methanol containing TEA followed by EDC addition. After 1 h, NHS was added and the mixture stirred for 3 h before adding DSPE. The mixture was stirred again for 24 h at room temperature. The product was dialyzed against deionized water and freeze-dried to obtain FA-PEG-DSPE conjugate. Conjugates were confirmed by Fourier transform infrared spectroscopy (FT-IR) (Vertey 70, Bruker, Germany). The lyophilized samples were mixed with KBr and prepared as pellets. The spectra were obtained from samples in the range of 400–4000 cm⁻¹ at room temperature.

5FU containing liposomes were prepared by thin film hydration method. Briefly, PC/cholesterol and PC/cholesterol/ FA-PEG-DSPE at the molar ratio of 2:1 and 2:1:0031, respectively were dissolved in chloroform. After solvent removal on a rotary evaporator (Heidolph, Germany), the thin lipid film was hydrated with 0.8 mL phosphate buffer saline (PBS, pH 7.4) containing 5FU (1.5 mg) by sonication in a water bath (Elma, Germany) for 30 min. In order to obtain liposomes of

a homogeneous size, the resulting liposomes were shear in a homogenizer (Heidolph, Germany) for another 5 min. Then, 5FU loaded liposomes were separated by centrifugation at 15000 rpm for 30 min (MPW-350R, Poland).

2.2. Characterizations of liposomes

2.2.1. Morphology and particle size determination

The morphology of liposomes was evaluated by transmission electron microscopy (TEM, LEO 906, Zeiss, Germany). A drop of dispersed liposome was placed onto a carbon-coated copper TEM grid and allowed to dry at room temperature before measurement. Particle size of liposomes was also determined using a particle sizer (QuDix, Scatterscope I system, Korea) before and after sonication in a water bath for 5 min to evaluate the impact of sonication on the nanoparticles size. All of measurements were performed at 25 °C. Prior to each measurement, samples were diluted with deionized water. Sonication was performed to prevent particles agglomeration and avoiding particle growth.

2.2.2. Determination of encapsulation efficiency (EE%)

The supernatant obtained after centrifuging liposomes was analyzed for the amount of un-entrapped 5FU using high performance liquid chromatography (HPLC, Waters, USA). The analysis was carried out on C₁₈ column (250 × 4 mm i.d., 5 μm) and the column temperature was set at 30 °C. The mobile phase was consisted of 0.02 M phosphate buffer pH 4 and methanol (70:30, V/V). Injection volume was 50 μL and the flow rate was 0.8 mL/min. Wavelength of detection was 260 nm and metronidazole was used as internal standard. The EE% was calculated according to eq. 1:

$$EE\% = 100 \frac{TD - FD}{TD} \quad (1)$$

where, TD is the amount of 5FU initially added to the formulation and FD is the amount of the free drug in the supernatant after centrifugation (Joshi et al., 2014).

2.2.3. Stability study of liposomes

The storage stability of the 5FU loaded liposomes were evaluated by monitoring the EE% and particle size at the beginning of the experiment and after 1 and 3 months. At the mentioned intervals, samples were resuspended in deionized water for assaying of EE% and particle size.

2.3. Cellular uptake

The intracellular uptake of liposomes was assayed by entrapment of CF dye in liposomes instead of 5FU that does not represent fluorescent property. CT26 cells were seeded onto 6-well plates and incubated for 24 h in the presence of 5% CO₂ and at 37 °C. After 24 h, the cells were treated by free CF and CF loaded targeted liposome and incubated for 4 h at 37 °C. After incubation, the cells were washed with cold PBS and fixed with 4% paraformaldehyde for 15 min. For distinction the green color of CF, the cell nucleus was further stained with 4, 6-diamidino-2-phenylindole (DAPI) for 10 min and then cells were washed with PBS before imaging. The intracellular uptake of CF in the cells was observed using fluorescent microscope (Olympus IX71, Japan).

2.4. In vitro cytotoxicity study

MTT assay was performed to evaluate cell viability. CT26 cells were grown at 37 °C, 5% CO₂ and 95% relative humidity in RPMI 1640 medium containing 10% FBS and 1% penicillin-streptomycin. Cells were seeded into 96-well plates at seeding density of 1 × 10⁴. After incubation for 24 h, the medium was replaced with fresh medium containing 5FU, liposomal 5FU and folate-liposomal 5FU at different concentrations (10, 15, 25, 35, 50 and 75 μM) for 48 h. After removing

the media, cells were incubated with solution MTT (5 mg/mL in PBS) at 37 °C for 4 h. Thereafter, DMSO (150 µL) was added in each well and shaken for 20 min. The absorbance of each plate was read at 570 nm using ELISA plate reader (BioRad, USA). Cellular viability was determined according to Eq. (2) and the half maximal inhibitory concentration (IC₅₀) was also calculated as cytotoxicity index.

$$\text{Cell viability\%} = 100 \frac{\text{Abs}_{\text{sample}}}{\text{Abs}_{\text{control}}} \quad (2)$$

2.5. Intracellular reactive oxygen species (ROS) production

ROS generation in cells was determined by using 2', 7'-dichlorofluorescein diacetate (DCFDA). DCFDA passively diffuses into cells and cleaves by esterases to non-fluorescent compound which further oxidizes by intracellular ROS into fluorescent 2', 7'-dichlorodihydrofluorescein (DCF) (Mulik et al., 2010). Briefly, cells at a density of 1×10^5 were seeded into 6-well plate and allowed to attach for 24 h. Then, the cells were treated with IC₅₀ dose of free 5FU and folate-liposomal 5FU for 1, 3, 24 and 48 h. After treatment, cells were washed with PBS and exposed to 10 µM DCFDA for 45 min at 37 °C. Fluorescence was monitored at excitation wavelength of 485 nm and emission wavelength of 530 nm using spectrofluorimeter (PerkinElmer, USA).

2.6. Hemolysis assay

The impact of liposomes on red blood cells (RBCs) was evaluated by a hemolysis assay test. Fresh blood was collected from male Wistar rats and centrifuged at 1500 rpm for 10 min. The RBCs were further washed three times with PBS. The suspension obtained (2%) was used for hemolysis study. Liposomes at different concentrations (0.1, 0.25 and 0.5 mg/mL) were added in RBCs suspension and incubated for 3 h at 37 °C. After that, the mixtures were centrifuged at 1500 rpm for 10 min. The supernatant was collected and the amount of hemoglobin released was determined by spectrophotometer (Biochrom WPA biowave II, England) at 540 nm. Double-distilled water was used as positive control and PBS was used as negative control. The hemolysis percentage was calculated according to Eq. (3):

$$\text{Hemolysis\%} = 100 \frac{A_s - A_{nc}}{A_{pc} - A_{nc}} \quad (3)$$

where, A_s is the absorbance of sample, A_{nc} is the absorbance of negative control and A_{pc} is the absorbance of positive control.

2.7. In vivo antitumor effect and histopathological study

In vivo experiments were performed with permission of the Animal Ethics Committee Jundishapur University of Medical Sciences, Ahvaz, Iran (ref no. IR.AJUMS.REC.1395.643). The BALB/c male mice were subcutaneously injected with 100 µL of cell suspension containing 1×10^6 CT26 cell in the right flank. After the tumor volume was reached to 100 mm³, the mice were randomly divided into three groups: control, 5FU and folate-liposomal 5FU. Different formulations of 5FU were given at the same dose of 20 mg/kg and administered via intraperitoneally in every other day (6 injections for period 12 of days). The tumor volume was measured by a caliper and calculated using the Eq. (4):

$$V = (W^2 \times L)/2 \quad (4)$$

where L and W are is the longest shortest diameter, respectively.

At the end of treatment (day 21), mice were sacrificed and the tumor, heart and kidney were dissected, fixed with 10% paraformaldehyde, embedded in paraffin and sectioned. The tissue slices were stained with hematoxylin and eosin (H&E) and observed using optical microscope (Olympus IX50, Japan).

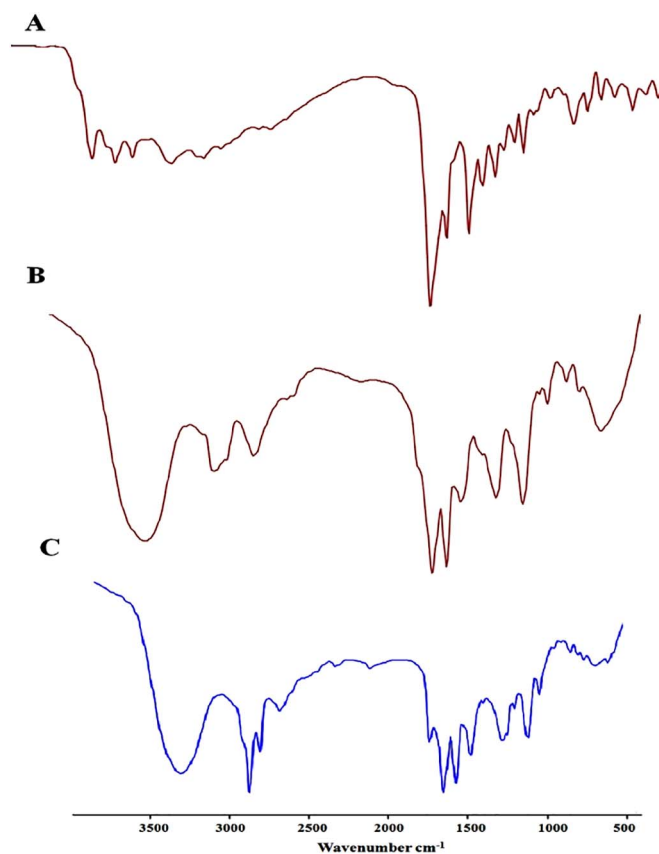


Fig. 1. FTIR spectra of A) folic acid, B) FA-PEG and C) FA-PEG-DSPE.

2.8. Statistical analysis

All the measurements were done in triplicate and data were expressed as mean \pm SD. One way ANOVA test was used for comparison of the results and the statistical significance was indicated by $p < 0.05$.

3. Results and discussion

The objective of the present study was to develop liposomal 5FU anchored with folic acid for their selective localization at cancer cells. Compared to the previous works, this is the first comprehensive study on the folate-liposomal 5FU regarding in vitro cellular uptake, cytotoxic study, ROS production, hemolysis assay, in vivo antitumor effect and histopathological study.

3.1. Characterizations of 5FU loaded liposomes

The FTIR spectra of FA, FA-PEG and FA-PEG-DSPE are shown in Fig. 1A–C. In FTIR spectra of Fig. 1B, the band at 1470 cm⁻¹ represents the stretching in backbone of aromatic ring of folic acid. The band at 2958 cm⁻¹ is corresponded to C–H stretching of aromatic ring of folic acid. The peak at 1103 cm⁻¹ indicates the presence of C–O group in the PEG. Moreover, the peak at 2961 cm⁻¹ is associated to the C–H groups of PEG. As shown in the Fig. 1C, absorbance peaks at 1468 and 1564 cm⁻¹ are related to aromatic C=C stretching vibrations rings in the folic acid. A sharp peak at 1178 cm⁻¹ is related to P=O stretching vibrations in DSPE. The bands at 1643 and 1736 cm⁻¹ are corresponded to the ester and amide (C=O) groups in the DSPE, respectively. The broad band at 3374 cm⁻¹ is attributed to OH acid groups on the ring of folic acid. The peaks at 2851 and 2919 cm⁻¹ represent the C–H stretching bands in the aliphatic structure of the PEG, FA and DSPE. Synthesis pathway of FA-PEG-DSPE and also preparation of liposomes are illustrated in Fig. 2A.

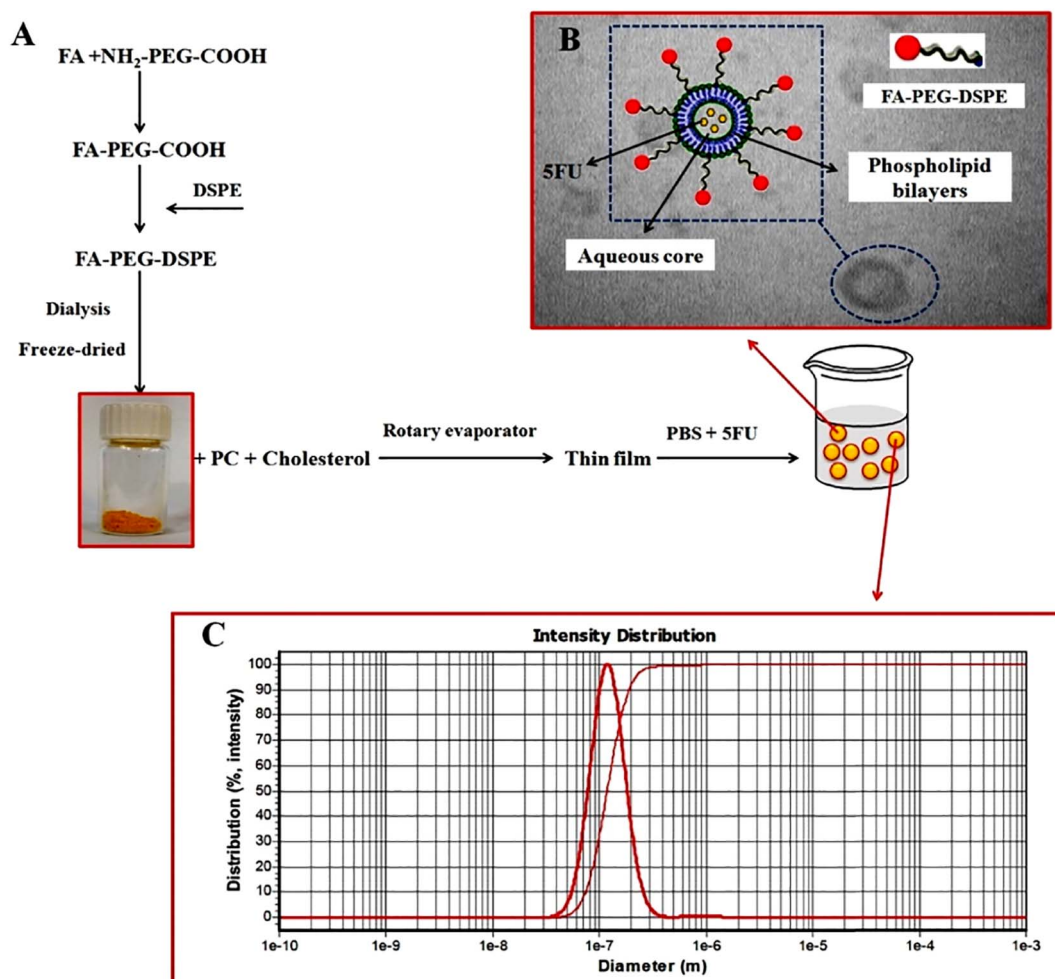


Fig. 2. A) Schematic illustration of synthesis pathway of FA-PEG-DSPE and preparation of liposomes, B) TEM image of liposomes and C) particle size distribution.

The amount of drug encapsulated in liposomes, particle size and stability of liposome are important parameters that should be considered during preparation of liposome as drug delivery systems (Pereira et al., 2016). EE% of 5FU in liposomes was found to be $67.88 \pm 1.84\%$. This encapsulation efficiency indicates that the liposomes are suitable as drug carriers. Liposomes were spherical in shape and were well dispersed as observed in the TEM image (Fig. 2B). The mean particle size of liposomes was 114.00 ± 4.58 nm and size distribution graph of liposomes are presented in Fig. 2C. There was no significant change in particle size after conjugation with FA. It is well known that the size of liposomes is a main factor for the tissue targeting. Larger liposomes are often taken up by phagocytes; while, small liposomes (100 to 200 nm) can penetrate easily in tumor tissue due to enhanced permeability and retention (EPR) effects (Nogueira et al., 2015; Shigehiro et al., 2014). Moreover, no significant difference was observed in the EE% and particle size of liposomes after 3 months, confirming the good physical stability of the prepared liposomes.

3.2. Cellular uptake

In the study, CF was selected as the fluorescent dye for labeling the liposomes. The selection of the dye was also based on the similarity of its nature (hydrophilicity) with 5FU. As shown in Fig. 3, the green fluorescence was very strong in cells which treated with CF loaded folate-targeted liposomes, indicating that a large amount of dye was accumulated in the cells compared to cells that were exposed to free CF. The results revealed the efficiently of targeted liposomes. Low bioavailability and low membrane permeability of hydrophilic drugs limit

their therapeutic efficacy. Entrapment of hydrophilic drugs in drug delivery systems such as liposomes can improve the delivery and bioavailability of the drugs (Eloy et al., 2014). On the other hand, increased intracellular uptake of drugs loaded in targeted liposomes may confirm the idea that folate-targeted liposomes are internalized in the cells via endocytosis (Zeng et al., 2014). While, drugs in solution form penetrate in the cells by passive diffusion; therefore, this difference may affect intracellular uptake of drugs (Mulik et al., 2010).

3.3. In vitro cytotoxicity study

MTT assay was performed to evaluate in vitro cytotoxicity of 5FU, liposomal 5FU and folate-liposomal 5FU. In the study CT26 cell line was selected as it overexpresses the FRs on surface (Benns et al., 2001). As shown in Fig. 4A, it was found that 5FU loaded targeted liposomes exhibited higher cytotoxicity than free drug and non-targeted liposomes ($p < 0.05$). The IC₅₀ values for 5FU, liposomal 5FU and folate-liposomal 5FU were 39.81, 37.15 and 12.02 μ M, respectively. In all formulations the viability of cells decreased with the increasing of the drug concentration. Also, as displayed in the Fig. 4A, no significant difference was found between cytotoxicity of 5FU and liposomal 5FU that may be a result of poor cellular internalization of non-targeted liposomes. Similar results were observed by Gupta et al. (2007) which showed that there was no significant difference between free 5FU and non-targeted liposomes on B16F10 melanoma cells. While, targeted liposomal 5FU with folic acid increased cytotoxicity of the drug significantly. Although, the IC₅₀ of folate-liposomal 5FU on cancer cell in their study was lower than IC₅₀ obtained in our study. This difference

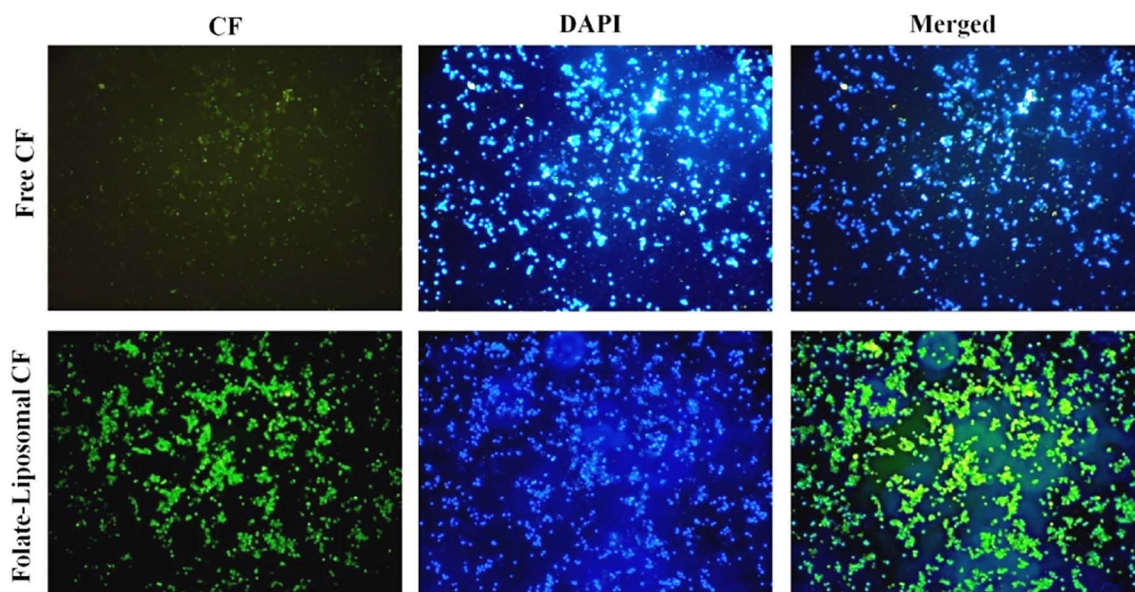


Fig. 3. Cellular uptake of free CF and CF loaded folate-targeted liposomes in cancer cells. (Left to right: green fluorescent signals are related to CF that is accumulated in the cytoplasm of the cells, the blue is corresponded to DAPI which is accumulated in the nuclei of cells, and final images at right show the merged CF and DAPI accumulation). (For interpretation of the references to color in this figure legend, the reader is referred to the web version of this article.)

may be related to the dissimilarity of cell lines used in the two studies (Gupta et al., 2007). The finding proves that targeted liposomes are more efficiently up taken by cancer cells than non-targeted liposomes. The results can be attributed to the presence of FA in the liposomes, which may facilitate the drug accumulation in the cells due to the presence of FRs on surface of cancer cells (Ai et al., 2017). The higher cytotoxicity of drug loaded targeted liposomes may be also related to the higher cellular uptake via endocytosis. On the other hand, the low particle size of NPs permits their accumulation in cells and retarded release of the drug, extends their action for a longer time period; while, due to its hydrophilicity, free 5FU in solution is poorly absorbed and washes out quickly (Mattos et al., 2016). The similar results were reported by Le et al. (2015). They found that no significant difference was between cytotoxicity of 5FU and 5FU loaded NPs on cancer cells. However, the cytotoxicity of folate-targeted NPs was significantly increased compared to free drug and non-targeted NPs. They also suggested that folate-targeted NPs may probably enter tumor cells by folate receptor-mediated endocytosis (Le et al., 2015). The effect of FAs blocking on the efficiency of folate- targeted NPs was reported in the study of Varshosaz et al. (2014). They observed that by addition of free folic acid to the folate-free culture medium of CT26 cells, cell viability was increased to $51.98 \pm 6.3\%$. These results indicated that free folic acid inhibited FR-dependent binding and uptake of NPs, which confirmed the uptake of folic acid targeted NPs by FR-mediated

endocytosis in cancer cells (Varshosaz et al., 2014). Lv et al. (2017) expressed that capsaicin loaded folate-targeted NPs exhibited a remarkably higher toxic effect compared to non-targeted NPs. Moreover, they demonstrated that anticancer effect of drug loaded-targeted NPs is attributed to the efficient cellular uptake of NPs via FRs-mediated endocytosis pathway which resulting in the higher amount of NP present in the cancer cells in comparison with non-targeted NPs (Lv et al., 2017). The present results are also in agreement with Zhang et al. (2016a, 2016b) observation which reported that cytotoxicity of etoposide loaded in folate-targeted NPs was significantly higher than non-targeted NPs and etoposide solution (Zhang et al., 2016b).

3.4. Evaluation of intracellular ROS production

It has been reported that 5FU significantly increase the generation of ROS in cancer cells (Liu et al., 2016). Increase of ROS in cells has been found as an activator of cell apoptotic signaling (Jin et al., 2016). Therefore, we evaluated the effect of 5FU and folate-liposomal 5FU on generation of ROS in time dependent manner. It should be mentioned that based on MTT results, no significant differences in cell viability were observed between 5FU and liposomal 5FU; therefore, evaluation of intracellular ROS production was only carried out for 5FU and folate-liposomal 5FU. It was found that folate-liposomal 5FU induced higher ROS with increasing in the time of treatment; while, in 5FU treated cells

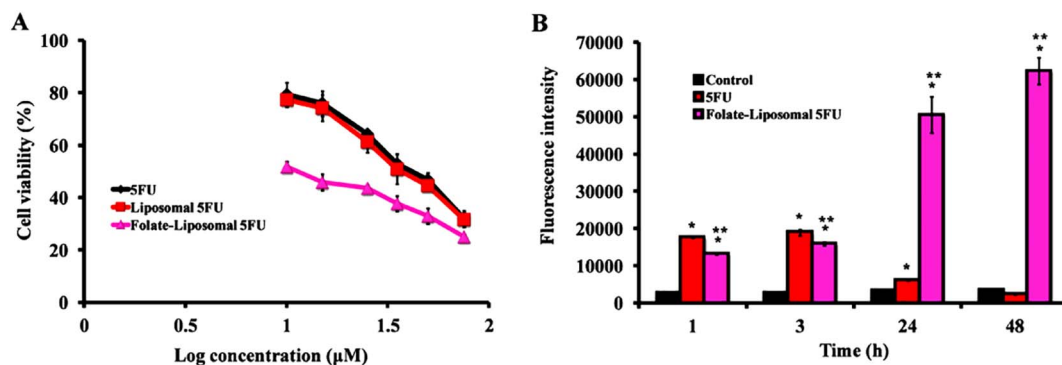


Fig. 4. A) cytotoxicity of different formulations of 5FU on CT26 cells and B) ROS production.

the ROS generation decreased after 24 h (Fig. 4B). The data obtained confirmed the results of cytotoxicity and cellular uptake study which exhibiting the increased generation of ROS with folate-liposomal 5FU, makes the encapsulated drug to be continuously release and increases uptake of targeted liposomes by FR-mediated endocytosis. The findings of present study confirm the results of Jin et al. (2016) which reported that folate-targeted chitosan NPs induced overproduction of ROS and resulted apoptosis pathway in MCF-7 cells.

In order to examine the contribution of ROS generation to folate-targeted NPs induced apoptosis, they co-cultured MCF-7 cells with these NPs and *N*-acetyl-L-cysteine (as a ROS inhibitor). They observed that *N*-acetyl-L-cysteine considerably reduced the capability of targeted NPs to inhibit cellular viability of cancer cells (Jin et al., 2016). Malhi et al. (2012) indicated that folate-liposomal doxorubicin significantly increased ROS production in cancer cells more than the free drug. They demonstrated that folic acid present on the surface of the liposomes improved the intra cellular delivery of doxorubicin and as a result increasing of ROS generation (Malhi et al., 2012). The findings of Fasehee et al. (2016) are also accordant with our results. They found that intracellular ROS level of cancer cells treated with disulfiram loaded folate-targeted NPs was more than free Disulfiram, indicating more disulfiram was transformed into the cells and induced higher ROS production (Fasehee et al., 2016). Considering these results, folate-liposomal 5FU induced death of cancer cells seems to correlate with ROS production.

3.5. Hemolysis assay

Hemo-compatibility assay is necessary to evaluate any possible hemolytic potential of liposomes with RBCs which determine their in vivo fate and influence their therapeutic efficacy (Raveendran et al., 2016). As displayed in Fig. 5A, there was no significant hemolysis caused by liposomes at different concentrations (below 5% of hemolysis induced by positive control), which indicating their good hemo-compatibility and further promised their application in vivo. Also, as shown in Fig. 5B, in the positive control (H₂O) and negative control (PBS) group, there was complete and non-significant hemolysis of RBCs, respectively. The results of Kuznetsova et al. (2012) study in this field are in accordance with our findings which reported that liposomes exhibited good hemotolerance (Kuznetsova et al., 2012). Similar results were reported by Clares et al. (2013). They indicated that liposomes can be considered as suitable delivery system for parenteral administration, because they exhibit a negligible effect on hemolysis (Clares et al., 2013). Bharti et al. (2017) also implied that liposomes revealed no significant hemolytic effect in RBCs (Bharti et al., 2017).

3.6. In vivo antitumor effect and histopathological study

At the end of treatment, the average volume of tumors was 1173.75,

210.00, and 88.75 mm³ for control, 5FU and folate-liposomal 5FU, respectively (Fig. 6A). According to the Fig. 6B, the tumor volumes of folate-liposomal 5FU groups were significantly smaller than free 5FU and control groups ($p < 0.05$). These results are in consistent with data obtained from in vitro cytotoxicity study, confirming that folate-targeted liposomes induced higher anticancer activity both in vitro and in vivo. Moreover, there was no difference in the body weights or change in feeding and movement between the treated and the control groups (data not shown). These findings support the results of Gupta et al. (2007) which showed that folate-liposomal 5FU had greater tumor-inhibitory effect than free drug (Gupta et al., 2007). The enhanced 5FU efficacy by using folate-targeted liposomes may be attributed to the passive and active targeting. Due to the leaky nature of the tumor-associated blood vessels, NPs can present higher permeability to tumor tissues based on their enhanced permeability and retention (EPR) effect (Mattos et al., 2016). Moreover, lack of lymphatic vessels around the tumor region reduces the exposure of other tissues to the drug which result reducing side effects (Mattos et al., 2016; Nair et al., 2011). As mentioned in the Section 3.1, the NPs with the size of 100 to 200 nm are more efficiently accumulated in solid tumors than normal tissues. In the present study, liposomes with about 114.00 nm effectively targeted cancer cells mainly due to the EPR effect in tumor tissues.

In the other hand, the higher antitumor activity of folate-liposomal 5FU might be due to high binding affinity of folate in the liposomes and FRs in the cancer cells which resulting in higher concentration and accumulation of the folate-targeted liposomes in tumors tissues (Wang and Kim, 2015). Our findings seem to agree with Jin et al. (2016) results. They reported that folate-targeted NPs had size about 100–200 nm which may easily internalized into cancer cells owing to EPR effect. Moreover, they found that folate-targeted NPs could be internalized in tumors tissues through FRs-mediated endocytosis pathway (Jin et al., 2016). The similar results have been reported by Le et al. (2015). They implied that the average tumor volumes of the mice, treated with entrapped 5FU in folate-targeted NPs were smaller than control groups. In addition, they observed that the uptake of targeted NPs into the cells was through FRs-mediated endocytosis (Le et al., 2015). The present results also confirm previous research of Zhang et al. (2016a, 2016b) which indicated that the higher anticancer activity of doxorubicin loaded folate-targeted NPs is related to the EPR effect and high binding affinity of folate conjugated NPs with FRs on surface of cancer cells (Zhang et al., 2016a). According to the finding of previous studies and our results, it can be concluded that effective antitumor activity of folate-liposomal 5FU may be associated with EPR effect, the presence of FA molecules on the surface of liposomes which further enhances their specific internalization in cancer cells and induction of apoptosis pathway (Fig. 7).

Histological analysis of heart and kidney showed the integrity of tissues structures and no obvious abnormality and no remarkable

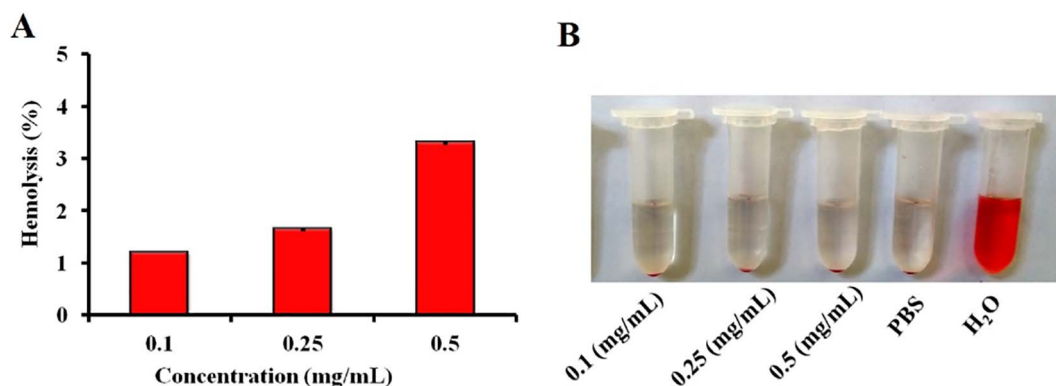


Fig. 5. Hemolysis assay: A) hemolysis (%) and B) image of RBCs treated with different concentrations of liposome, PBS (–) and H₂O (+).

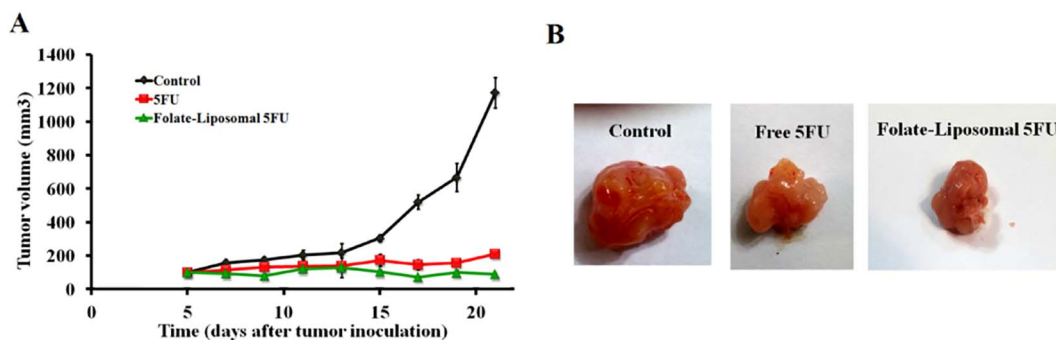


Fig. 6. Evaluation of tumor growth inhibition of free 5FU and folate-liposomal 5FU: A) tumor volume, B) image of solid tumor.

pathological change was observed (Fig. 8). Also, as can be seen in Fig. 8, the folate-liposomal 5FU treated group exhibited lower cell density in tumor tissue compared with control group. These results indicated that targeted liposomes could effectively inhibit tumor growth. Based on these results, it can be concluded that the folate-targeted liposomes can be employed as carrier for anticancer agents in cancer therapy.

4. Conclusion

The results of cellular uptake showed that targeted liposome

internalized much more CF than CF solution. Compared with 5FU, targeted liposome revealed higher cytotoxic activity on cancer cells. Moreover, targeted liposomes significantly enhanced ROS level in cancer cells. Hemolysis assay confirmed that liposomes were hemo-compatible which supporting its use as intravenous injection. Folate-liposomal 5FU exhibited high in vivo antitumor activity as compared with free drug. Selective and enhanced accumulation of targeted liposomes in cancer cells may be due to combined EPR and more selective receptor-mediated endocytosis. The results of histopathological analysis displayed that targeted liposomes did not show any obvious damage to heart and kidney. According to the results, folate-targeted liposomes

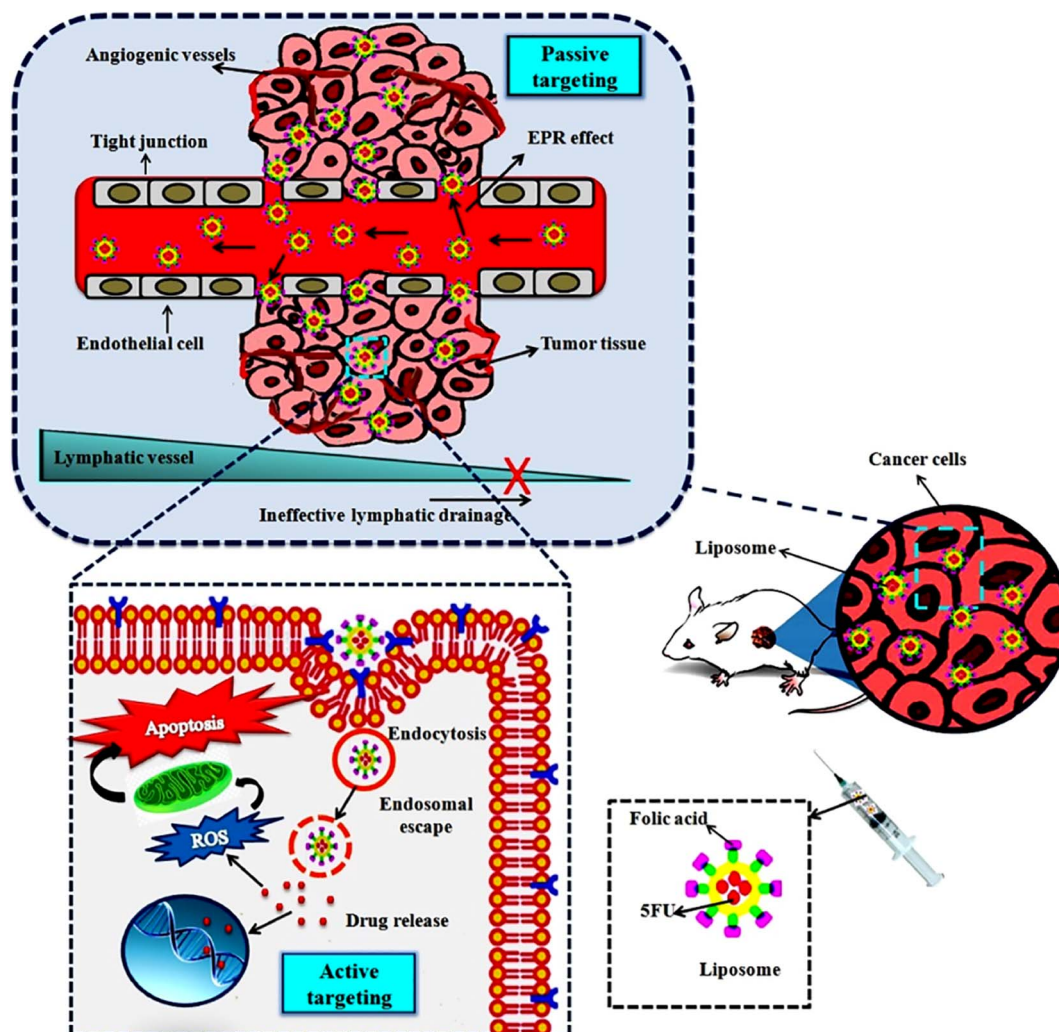


Fig. 7. Schematic representation of antitumor activity of folate-liposomal 5FU in cancer cells.

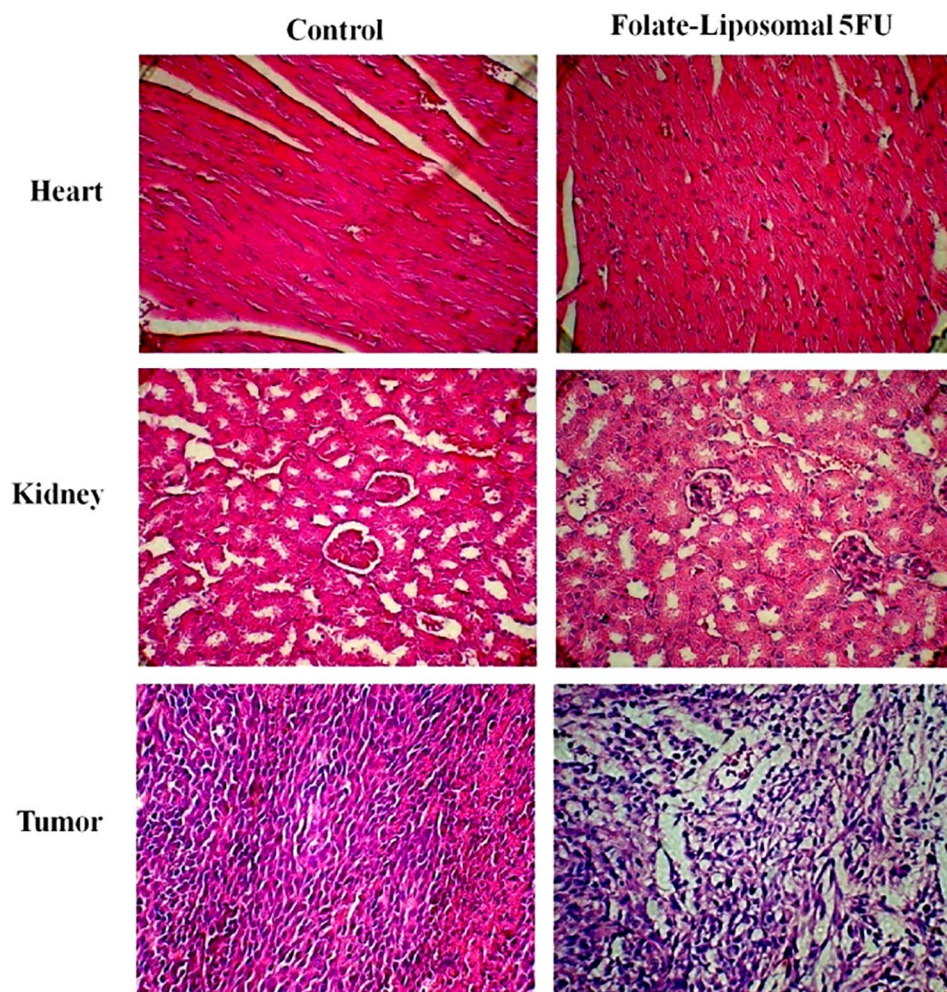


Fig. 8. Histopathologic images of heart, kidney and tumor sections with H&E staining of control and treated with folate-liposomal 5FU groups ($\times 300$ magnification).

might be a promising approach for treatment of colon cancer.

Acknowledgment

The work was financially supported by Nanotechnology Research Center, Ahvaz Jundishapur University of Medical Sciences, Ahvaz, Iran (grant No. 111) and Iran National Science Foundation (grant No. INSF-93032941). Also, the authors gratefully thank Dr. Esrafil Mansouri for his cooperation in histopathological analysis.

Conflict of interest

The authors report no conflict of interest.

References

- Ai, J.W., Liu, B., Liu, W.D., 2017. Folic acid-tagged titanium dioxide nanoparticles for enhanced anticancer effect in osteosarcoma cells. *Mater. Sci. Eng., C* 76, 1181–1187.
- Benns, J.M., Maheshwari, A., Furgeson, D.Y., Mahato, R.I., Kim, S.W., 2001. Folate-PEG-folate-graft-polyethylenimine-based gene delivery. *J. Drug Target.* 9, 123–139.
- Bharti, R., Dey, G., Banerjee, I., Dey, K.K., Parida, S., Kumar, B.N., Das, C.K., Pal, I., Mukherjee, M., Misra, M., Pradhan, A.K., Emdad, L., Das, S.K., Fisher, P.B., Mandal, M., 2017. Somatostatin receptor targeted liposomes with Diacerein inhibit IL-6 for breast cancer therapy. *Cancer Lett.* 388, 292–302.
- Chen, Y., Minh, L.V., Liu, J., Angelov, B., Drechsler, M., Garamus, V.M., Willumeit-Romer, R., Zou, A., 2016. Baicalin loaded in folate-PEG modified liposomes for enhanced stability and tumor targeting. *Colloids Surf. B: Biointerfaces* 140, 74–82.
- Cheng, M., He, B., Wan, T., Zhu, W., Han, J., Zha, B., Chen, H., Yang, F., Li, Q., Wang, W., Xu, H., Ye, T., 2012. 5-fluorouracil nanoparticles inhibit hepatocellular carcinoma via activation of the p53 pathway in the orthotopic transplant mouse model. *PLoS One* 7, e47115.
- Clares, B., Biedma-Ortiz, R.A., Saez-Fernandez, E., Prados, J.C., Melguizo, C., Cabeza, L., Ortiz, R., Arias, J.L., 2013. Nano-engineering of 5-fluorouracil-loaded magnetoliposomes for combined hyperthermia and chemotherapy against colon cancer. *Eur. J. Pharm. Biopharm.* 85, 329–338.
- Deshpande, P.P., Biswas, S., Torchilin, V.P., 2013. Current trends in the use of liposomes for tumor targeting. *Nanomedicine (London, England)* 8, 1509–1528.
- Eloy, J.O., Claro de Souza, M., Petrilli, R., Barcellos, J.P., Lee, R.J., Marchetti, J.M., 2014. Liposomes as carriers of hydrophilic small molecule drugs: strategies to enhance encapsulation and delivery. *Colloids Surf. B: Biointerfaces* 123, 345–363.
- Fasehee, H., Dinarvand, R., Ghavamzadeh, A., Esfandyari-Manesh, M., Moradian, H., Faghihi, S., Ghaffari, S.H., 2016. Delivery of disulfiram into breast cancer cells using folate-receptor-targeted PLGA-PEG nanoparticles: in vitro and in vivo investigations. *J. Nanobiotechnol.* 14, 32.
- Gao, Y., Li, Z., Xie, X., Wang, C., You, J., Mo, F., Jin, B., Chen, J., Shao, J., Chen, H., Jia, L., 2015. Dendrimeric anticancer prodrugs for targeted delivery of ursolic acid to folate receptor-expressing cancer cells: synthesis and biological evaluation. *Eur. J. Pharm. Sci.* 70, 55–63.
- Gupta, Y., Jain, A., Jain, P., Jain, S.K., 2007. Design and development of folate appended liposomes for enhanced delivery of 5-FU to tumor cells. *J. Drug Target.* 15, 231–240.
- Jin, H., Pi, J., Yang, F., Jiang, J., Wang, X., Bai, H., Shao, M., Huang, L., Zhu, H., Yang, P., Li, L., Li, T., Cai, J., Chen, Z.W., 2016. Folate-chitosan nanoparticles loaded with Ursolic acid confer anti-breast cancer activities in vitro and in vivo. *Sci. Rep.* 6, 30782.
- Joshi, G., Kumar, A., Sawant, K., 2014. Enhanced bioavailability and intestinal uptake of Gemcitabine HCl loaded PLGA nanoparticles after oral delivery. *Eur. J. Pharm. Sci.* 60, 80–89 (Aug 18).
- Kuznetsova, N.R., Sevrin, C., Lespiau, D., Bovin, N.V., Vodovozova, E.L., Meszaros, T., Szebeni, J., Grandfils, C., 2012. Hemocompatibility of liposomes loaded with lipophilic prodrugs of methotrexate and melphalan in the lipid bilayer. *J. Control. Release* 160, 394–400.
- Laha, D., Pramanik, A., Chattopadhyay, S., Dash, S.k., Roy, S., Pramanik, P., Karmakar, P., 2015. Folic acid modified copper oxide nanoparticles for targeted delivery in vitro and in vivo systems. *RSC Adv.* 5, 68169–68178.
- Le, V.M., Wang, J.J., Yuan, M., Nguyen, T.L., Yin, G.F., Zheng, Y.H., Shi, W.B., Lang, M.D., Xu, L.M., Liu, J.W., 2015. An investigation of antitumor efficiency of novel sustained and targeted 5-fluorouracil nanoparticles. *Eur. J. Med. Chem.* 92, 882–889.
- Liu, M.P., Liao, M., Dai, C., Chen, J.F., Yang, C.J., Liu, M., Chen, Z.G., Yao, M.C., 2016. *Sanguisorba officinalis* L synergistically enhanced 5-fluorouracil cytotoxicity in

- colorectal cancer cells by promoting a reactive oxygen species-mediated, mitochondria-caspase-dependent apoptotic pathway. *Sci. Rep.* 6, 34245.
- Lv, L., Zhuang, Y.X., Zhang, H.W., Tian, N.N., Dang, W.Z., Wu, S.Y., 2017. Capsaicin-loaded folic acid-conjugated lipid nanoparticles for enhanced therapeutic efficacy in ovarian cancers. *Biomed. Pharmacother.* 91, 999–1005.
- Malhi, S.S., Budhiraja, A., Arora, S., Chaudhari, K.R., Nepali, K., Kumar, R., Sohi, H., Murthy, R.S., 2012. Intracellular delivery of redox cyclers-doxorubicin to the mitochondria of cancer cell by folate receptor targeted mitocancerotropic liposomes. *Int. J. Pharm.* 432, 63–74.
- Mattos, A.C., Altmeyer, C., Tominaga, T.T., Khalil, N.M., Mainardes, R.M., 2016. Polymeric nanoparticles for oral delivery of 5-fluorouracil: formulation optimization, cytotoxicity assay and pre-clinical pharmacokinetics study. *Eur. J. Pharm. Sci.* 84, 83–91.
- Mulik, R.S., Monkkonen, J., Juvonen, R.O., Mahadik, K.R., Paradkar, A.R., 2010. Transferrin mediated solid lipid nanoparticles containing curcumin: enhanced in vitro anticancer activity by induction of apoptosis. *Int. J. Pharm.* 398, 190–203.
- Nair, K.L., Jagadeeshan, S., Nair, S.A., Kumar, G.S., 2011. Biological evaluation of 5-fluorouracil nanoparticles for cancer chemotherapy and its dependence on the carrier, PLGA. *Int. J. Nanomedicine* 6, 1685–1697.
- Nogueira, E., Gomes, A.C., Preto, A., Cavaco-Paulo, A., 2015. Design of liposomal formulations for cell targeting. *Colloids Surf. B: Biointerfaces* 136, 514–526.
- Pereira, S., Egbu, R., Jannati, G., Al-Jamal, W.T., 2016. Docetaxel-loaded liposomes: the effect of lipid composition and purification on drug encapsulation and in vitro toxicity. *Int. J. Pharm.* 514, 150–159.
- Raveendran, R., Bhuvaneshwar, G.S., Sharma, C.P., 2016. Hemocompatible curcumin-dextran micelles as pH sensitive pro-drugs for enhanced therapeutic efficacy in cancer cells. *Carbohydr. Polym.* 137, 497–507.
- Shigehiro, T., Kasai, T., Murakami, M., Sekhar, S.C., Tominaga, Y., Okada, M., Kudoh, T., Mizutani, A., Murakami, H., Salomon, D.S., Mikuni, K., Mandai, T., Hamada, H., Seno, M., 2014. Efficient drug delivery of paclitaxel glycoside: a novel solubility gradient encapsulation into liposomes coupled with immunoliposomes preparation. *PLoS One* 9, e107976.
- Shmeeda, H., Mak, L., Tzemach, D., Astrahan, P., Tarshish, M., Gabizon, A., 2006. Intracellular uptake and intracavitary targeting of folate-conjugated liposomes in a mouse lymphoma model with up-regulated folate receptors. *Mol. Cancer Ther.* 5, 818–824.
- Varshosaz, J., Hassanzadeh, F., Sadeghi-Aliabadi, H., Firozian, F., 2014. Uptake of Etoposide in CT-26 Cells of Colorectal Cancer Using Folate Targeted Dextran Stearate Polymeric Micelles.
- Wang, M., Kim, J.-C., 2015. In vivo tumor-suppressing efficacy and cell internalization of doxorubicin loaded in liposomes bearing folate. *J. Drug Delivery Sci. Technol.* 30, 190–198.
- Wang, C., Feng, L., Yang, X., Wang, F., Lu, W., 2013. Folic acid-conjugated liposomal vincristine for multidrug resistant cancer therapy. *Asian J. Pharm. Sci.* 8, 118–127.
- Yin, J.J., Sharma, S., Shumyak, S.P., Wang, Z.X., Zhou, Z.W., Zhang, Y., Guo, P., Li, C.Z., Kanwar, J.R., Yang, T., Mohapatra, S.S., Liu, W., Duan, W., Wang, J.C., Li, Q., Zhang, X., Tan, J., Jia, L., Liang, J., Wei, M.Q., Li, X., Zhou, S.F., 2013. Synthesis and biological evaluation of novel folic acid receptor-targeted, beta-cyclodextrin-based drug complexes for cancer treatment. *PLoS One* 8, e62289.
- Zeng, X., Morgenstern, R., Nyström, A.M., 2014. Nanoparticle-directed sub-cellular localization of doxorubicin and the sensitization breast cancer cells by circumventing GST-mediated drug resistance. *Biomaterials* 35, 1227–1239.
- Zhang, C., Zhang, Z., Zhao, L., 2016a. Folate-decorated poly(3-hydroxybutyrate-co-3-hydroxyoctanoate) nanoparticles for targeting delivery: optimization and in vivo antitumor activity. *Drug Deliv.* 23, 1830–1837.
- Zhang, S., Lu, C., Zhang, X., Li, J., Jiang, H., 2016b. Targeted delivery of etoposide to cancer cells by folate-modified nanostructured lipid drug delivery system. *Drug Deliv.* 23, 1838–1845.